Springer

KSME

Journal of Mechanical Science and Technology 31 (9) (2017) 4345~4351
www.springerlink.com/content/1738-494x(Print)/1976-3824(Online)
DOI 10.1007/s12206-017-0833-6

A study of the current density analysis for two type method on the invar alloy in electrochemical machining†

Seung-Geon Choi[1], Seong-Hyun Kim[1], Woong-Kirl Choi[1] and Eun-Sang Lee[2,*]

[1]*School of Mechanical Engineering, Inha Univ., 253 Yonghyun-Dong, Nam-Gu, Incheon, Korea*
[2]*Department of Mechanical Engineering, Inha Univ., 253, Yonghuyn-Dong, Nam-Gu, Incheon, Korea*

(Manuscript Received December 9, 2016; Revised March 30, 2017; Accepted May 10, 2017)

Abstract

Invar alloy is important material used for the OLED (Organic light emitting diode) shadow-mask in the mobile display industry due to its characteristics of smallest thermal expansion coefficient. Consumers in modern society demand higher display resolution. Electrochemical machining is one of the methods for obtained these high-resolution requirements. Electrochemical machining is a non-contact method that has advantages regarding defects like thermal strain and micro burrs compared to other non-conventional machining methods. For precision electrochemical machining using different shape electrodes, the current density should be controlled precisely. The purpose of this study is to apply the FEM (Finite elements method) analysis in order to investigate the current density in the electrochemical machining. And the current density distribution between invar alloy and electrode are carried out with shape electrode type and micro array film type under the same conditions by simulation methods. FEM analysis results show that using shape electrode type, current density distribution is very concentrated. And also by micro array pattern film, desired current density which is needed for electrochemical machining could be obtained easily. More precise electrochemical machining can be available by controlling the current density between the suitable type and invar alloy.

Keywords: Invar alloy; Current density; Electrochemical machining; Shape electrode type; Micro array film type

---

1. Introduction

Invar alloy is important material used for the OLED (Organic light emitting diode) shadow-mask in the mobile display industry due to its characteristics of smallest thermal expansion coefficient. Invar alloy exhibits a very low coefficient of linear expansion at room temperature and does not change its length even when the temperature changes. Micro-scale and complex shapes of invar alloy are often needed [1, 2]. Particularly, shadow masks must have fine and precise patterns.

In a general machining, micro-pattern processing is difficult. Non-traditional machining methods that have been researched for smart materials include laser machining, electro-discharge machining, MR fluid machining, etching, and electrochemical machining [3, 4]. Electrochemical machining can be used without stressing or transmuting the material through non-contact machining between the tool and workpiece using metal dissolution by electrochemical reaction. Method for processing a micro pattern on a workpiece has been continuing research. In electrochemical machining, the material and an electrode with a specific shape are placed in an electrolyte. Then, electrochemical dissolution of the material is generated by the electrode after current is applied to the material, which is connected to an anode (+), and to the tool electrode, which is connected to a cathode (-). An oxidization-deoxidization process occurs between the material and tool electrode.

It is difficult to machine complex shapes with normal machining, but it can be done with electrochemical machining, with which machining deformation does not occur. A micro-array pattern can be machined by electrochemical machining on Invar alloy. Electrochemical machining can be done with a many-shape electrode for drilling holes or with a through-mask. Researchers have focused on using multiple electrodes. Most papers focus on processing stainless steel. However, the Invar alloys used in a shadow mask are much thinner [5-7]. Therefore, it is not easy to machine micro-patterns.

In the present study, two methods for processing Invar alloy were compared. First, the 2D electric field was analyzed. The electric field is very important in electrochemical machining. We also compared the methods while changing the electrode gap size. From the shape of the electrode, we confirmed the field on the workpiece. Second, we compared the 3D current density. The current density distribution between the Invar alloy and electrode was studied using a shaped electrode and an array film electrode under the same conditions in simula-

*Corresponding author. Tel.: +82 32 860 7308
E-mail address: leees@inha.ac.kr
† Recommended by Associate Editor Taesung Kim

Table 1. Boundary condition of 2D analysis.

Conditions	Value
Voltage	30 V
Electrolyte	NaCl
Electrode gap	0.1, 0.2, 0.3, 0.4, 0.5 mm
Workpiece	Invar alloy

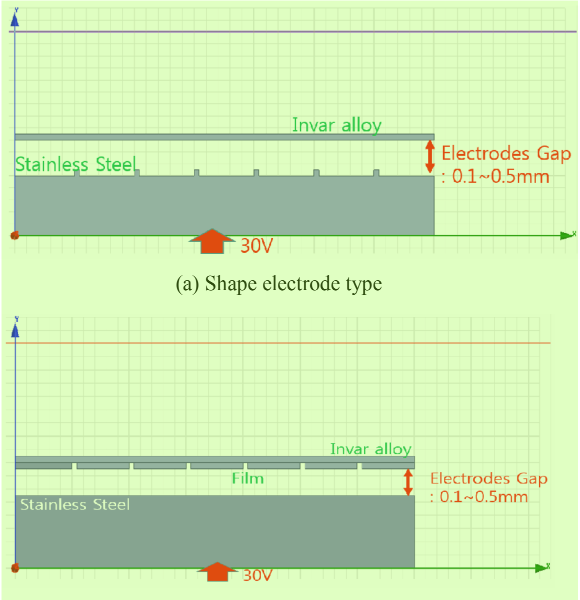

Fig. 1. 2D modeling and boundary condition.

tions using the Finite element method (FEM). Finally, the alloy was machined using different electrode types. The machining results and FEM results were compared [8].

2. 2D electric field analysis

In electrochemical machining, the electric field is the processing due to the electrical effect [9]. The electric field was determined for the two types of electrochemical machining, which were modeled for electric field analysis as shown in Table 1. Electrode gap was in 0.1, 0.2, 0.3, 0.4 and 0.5 mm. Voltage condition was 30 V and the analysis was conducted in the same condition. Also, the electrical properties of Invar alloy were input. The analysis tool was Maxwell, which was used to simulate the electric field of the invar alloy analysis for the different type.

Fig. 1 shows the 2D modeling and boundary condition and material property. Fig. 1(a) shows the micro electrode size of 0.05 mm and Fig. 1(b) shows the micro pattern film size of 0.05 mm. The electric field generated on the work was determined so that voltage would flow through the back of the electrode. Voltage enters the back of the electrode at 30 V after passing through the front of the invar alloy. Electrode gap was 0.1 mm~0.5 mm by changes to also with the analysis. The material property of electrode was stainless steel material

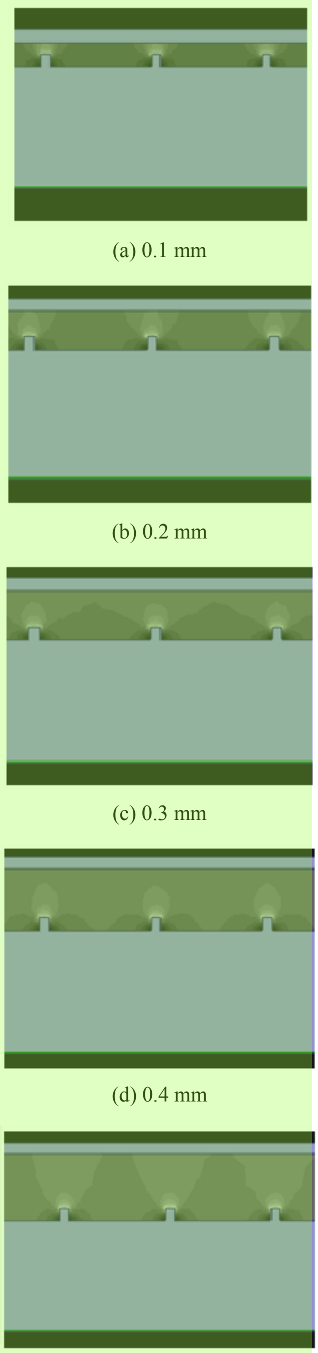

Fig. 2. 2D electric field analysis of shape electrode type.

property of workpiece was invar alloy and material property of array pattern film was insulation materials.

Fig. 2 shows the 2D electric field analysis of 6-shaped electrodes. Electrode gap was 0.1 mm~0.5 mm by changes to also with the analysis. The electric field of the electrode gap 0.1 mm was the most significant at the electrode edges at 5.2246e+005 V/m and the average electric field in the gap was 1.3062e+005 V/m. In addition, the electric field is radial value to 2.938e+005 V/m between the invar alloy and electrode. The electric field of the electrode gap 0.3 mm was the most significant at the electrode edges at 2.0278e+005 V/m and the average electric field in the gap was 8.871e+004 V/m. The electric field is radial value to 1.2674e+005 V/m between the invar alloy and electrode.

The electric field of the electrode gap 0.5 mm was the most significant at the electrode edges at 1.1873e+005 V/m. The average electric field in the gap was 5.1947e+004 V/m and the electric field is radial value to 5.9367e+004 V/m between the invar alloy and electrode. It is seen that the electric field was generated in a radial direction from the electrode projection. Current in the electrode shape is affected the surface of the workpiece for the electric field are overlapped is generated. It is difficult to process the desired shape by nested current.

Fig. 3 shows the 2D electric field analysis of array film type. Electrode gap was 0.1 mm~0.5 mm by changes to also with the analysis. The electric field of the electrode gap 0.1 mm was the average electric field in the gap was 2.0837e+004 V/m, and electric field in the pattern hole was 2.9159e+005 V/m. Analysis of the results when the electrode-gap 0.1 mm, the color between the gap is displayed in dark grey. What this means is that the overall electric field is concentrated in the analysis result of electrode gap. In addition, the largest electric field was generated at the edge of the electrode. The electric field of the electrode gap 0.3 mm was the average electric field in the gap was 1.6878e+004 V/m and electric field in the pattern hole was 2.5307e+005 V/m. Analysis of the results when the electrode-gap 0.3 mm, the color between the gap is displayed in dark grey. The color of the overall ratio between the electric field can be seen that the changed to light grey by the electrode gap was increased.

The electric field with a gap of 0.5 mm was also the average electric field in the gap (1.3316e+005 V/m). The electric field of the pattern hole was 1.9975e+004 V/m. The color between the gap is light grey. The electric field value appears to be low in this case. All of the results in Fig. 3 show that the largest electric field is at the edge of the electrode. In addition, all results show that the color of the pattern hole is light grey. When the gap was changed in the pattern, the electric field increased [10].

3. 3D current density analysis

Current density is a very important parameter in electrochemical machining. The current density was determined for the two types of electrochemical machining. Electrode gap was in 0.5, 0.25, 0.2, 0.15 and 0.1 mm and voltage condition was 30 V and the analysis was conducted in the same condition. Also, the electrical properties of Invar alloy were input. The 3D modeling tool was Solidworks, which was simplified to smooth analysis. The analysis tool was Ansys workbench, which was used to simulate the current density for the different electrodes for the invar alloy analysis.

Fig. 4 shows the 3D modeling and boundary condition and material property. Fig. 4(a) shows the 6x6 shape electrode and electrode size of 0.05 mm and Fig. 4(b) shows the 6x6 micro pattern film size of 0.05 mm. The current density generated on the work was determined so that voltage would flow through the back of the electrode. Voltage enters the back of the electrode at 30 V after passing through the front of the invar alloy. Electrode gap was 0.1 mm~0.5 mm by changes to also with the analysis. The material property of electrode was stainless steel, material property of workpiece was invar alloy and material property of micro array pattern film was insulation mate-

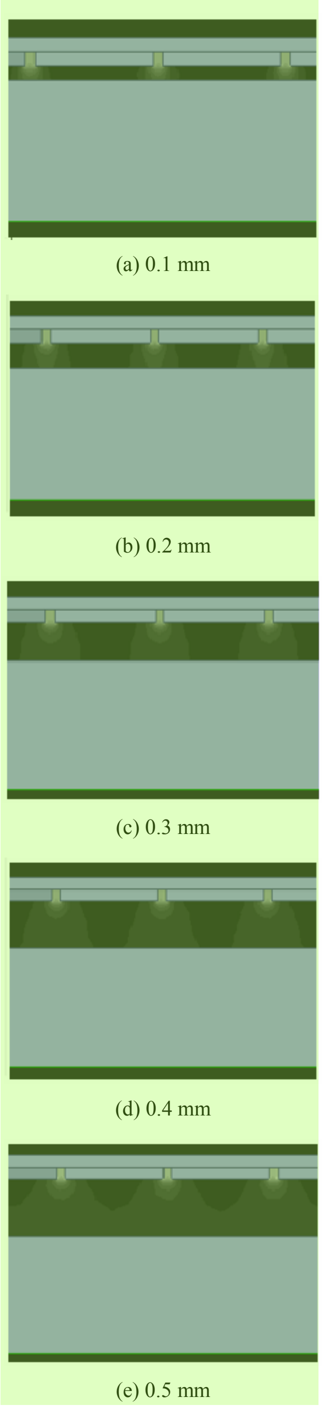

Fig. 3. 2D electric field analysis of array film type.

Table 2. Boundary condition of 2D analysis.

Conditions	Value
Voltage	30 V
Electrolyte	NaCl
Electrode gap	0.5, 0.25, 0.2, 0.15, 0.1 mm
Workpiece	Invar alloy

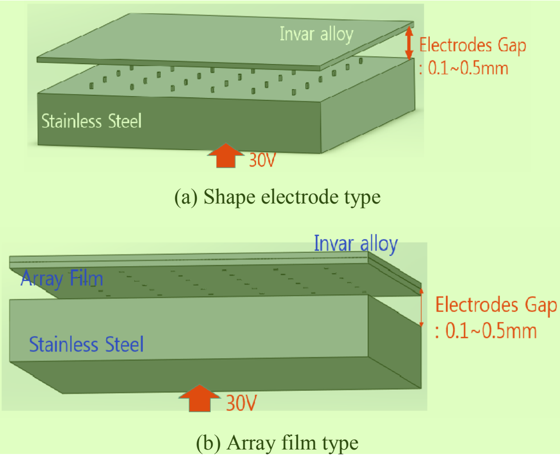

Fig. 4. 3D modeling and boundary condition.

rials. The precise analysis was performed with a mesh size of 0.1 mm and the analysis was the same for all conditions except for the electrode gap.

Fig. 5 shows the 3D current density analysis of 6x6 shape electrode. The size of electrode projection 0.05 mm x 0.08 mm and a 1 mm gap on each projection. Fig. 5(a) shows the current density analysis of the electrode gap was 0.5 mm. The current density was highest at the electrode projections at 1263.1 A/cm^2. When electrode gap was 0.5 mm, the current density at the electrodes is a phenomenon that occurs does not reach the workpiece. So that next the analysis, the performed electrode gap was to a difference of 0.05 mm. The current density of the electrode-gap 0.25 mm was the most significant at the electrode projection at 2313.3 A/cm^2 and the electrode-gap 0.2 mm was the most significant at the electrode projection at 3120.8 A/cm^2. The current density of the electrode gap 0.15 mm was the most significant at the electrode projection at 3153.7 A/cm^2 and the electrode gap 0.1 mm was the most significant at the electrode projection at 7332.3 A/cm^2. The analysis results, it was shown in the greatest current density at the electrode projection. Because invar alloy with the nearest, the current is concentrated. This is consistent with 2D analysis.

Fig. 6 shows the 3D current density analysis of 6x6 micro array film. The size of film pattern 0.05 mm x 0.08 mm and a 1 mm gap on each pattern. The same as the micro electrode was electrode gap in 0.5 mm, 0.25 mm, 0.2 mm, 0.15 mm, 0.1 mm. Fig. 6(a) shows the current density analysis of the electrode gap was 0.5 mm. The greatest current density was 371.78 A/cm^2 at the edge of the electrode. But the current density was not confirmed the pattern. the next electrode gap

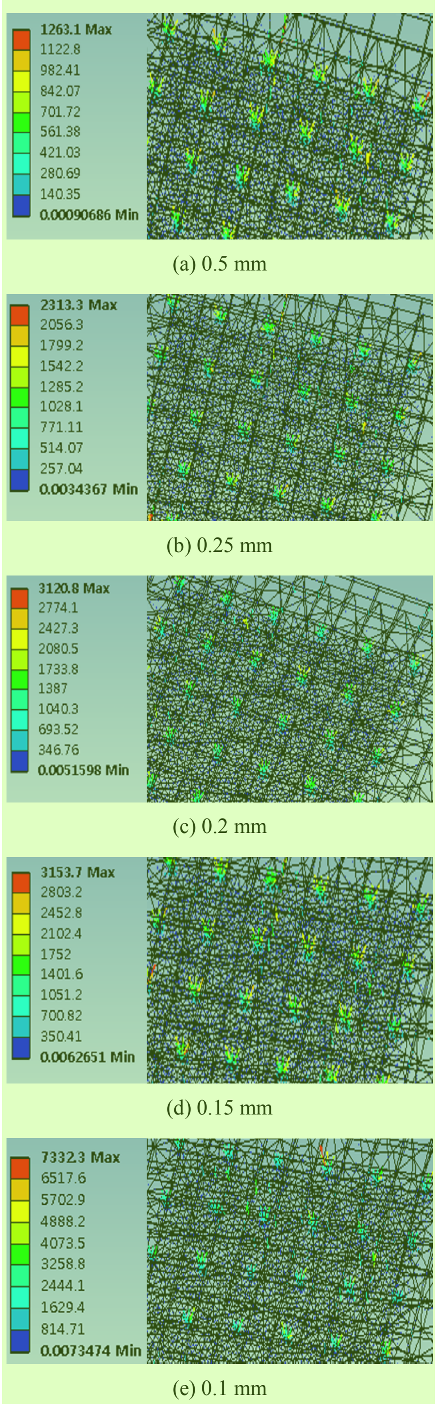

Fig. 5. 3D analysis of shape electrode type.

conditions were the same conditions from the shape electrode type. The current density of the electrode-gap 0.25 mm was the most significant at the electrode edge at 489.77 A/cm^2 and the electrode gap 0.2 mm was the most significant at the electrode edge at 441.12 A/cm^2. But, it is the current density was not confirmed at the pattern. The current density of the electrode-gap 0.15 mm was the most significant at the electrode edge at 462.46 A/cm^2 and the electrode gap 0.1 mm was the most significant at the electrode edge at 505.27 A/cm^2. Even if

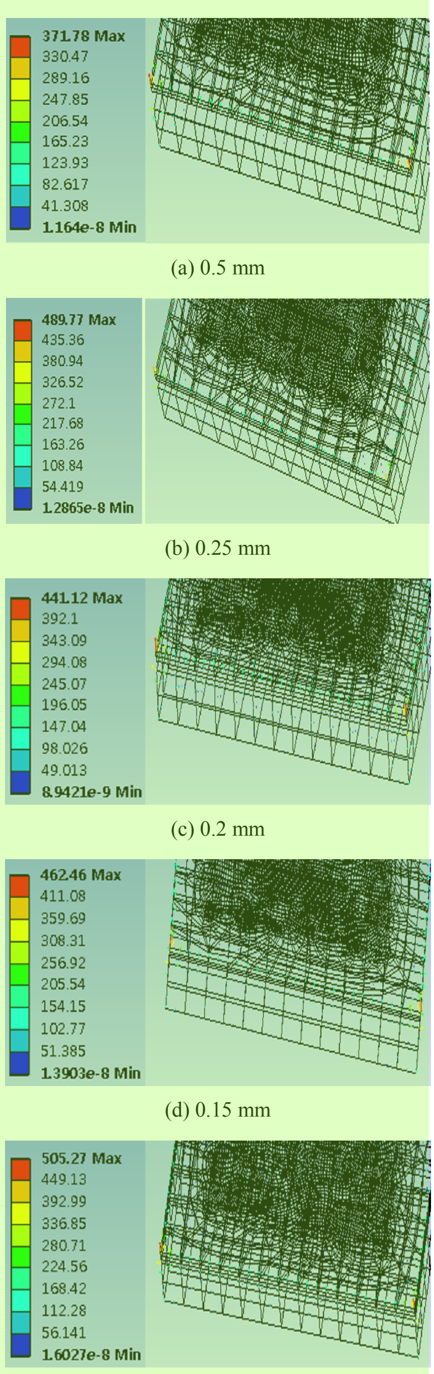

(a) 0.5 mm

(b) 0.25 mm

(c) 0.2 mm

(d) 0.15 mm

(e) 0.1 mm

Fig. 6. 3D current density analysis of array film type.

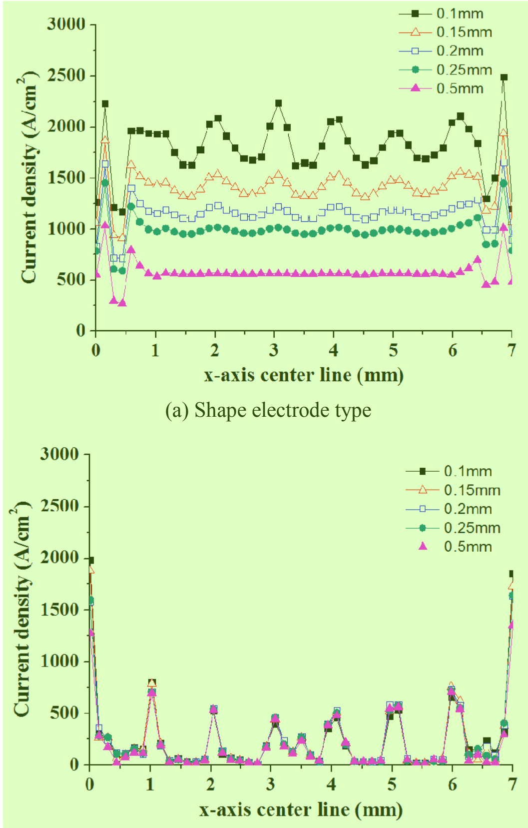

(a) Shape electrode type

(b) Array film type

Fig. 7. Current density graph in x-axis center line.

the electrode gap is reduced, the current density was not confirmed at the pattern. Such as the result of 2D analysis and 3D analysis, the pattern is determined that the low current generated. In order to determine the current density of the invar alloy surface, the center of surface was measured.

Fig. 7 shows the current density graph for the x-axis center line of the workpiece surface. Fig. 7(a) shows the current density result for the 6x6 shape electrode. For an electrode gap of 0.5 mm, the current density is distributed uniformly. With gaps of 0.25 to 0.15 mm, the graph showed peaks at the electrode locations. It can be seen that the magnitude at the electrode gaps was reduced because the current density was increased. However, if the electrodes were too close, the current density was not constant. Also, the current value is higher than that in Fig. 7(b).

Fig. 7(b) shows the current density results using the array film electrode. There was constant current density, regardless of the electrode gap. Because the micro-pattern hole was small, the magnitude of the current density was constant. Also, the magnitude of the current density applied to each of the holes is not constant. The shape electrode has higher current density than the array film. Due to the insulation, less current reaches the Invar surface.

4. Experiment

Based on the 2D and 3D analysis result, the experiments were carried out in order to know the optimal maching methods. Table 2 shows the experiment condition. Fig. 8 shows the electrochemical machining experiment of invar alloy. The electrode that was to be used as a tool was connected to the cathode (−), and a jig that was connected to a copper wire was connected to the anode (+). Fixing condition is a voltage and the electrolytic solution. The voltage was 30 V and the electrolyte was 0.1 mol NaCl. The experiment

Table 3. Machining parameters of experiment.

Conditions	Value
Voltage	30 V
Electrolyte	0.1 mol NaCl
Machining time	30 s
Electrode gap	0.1, 0.3, 0.5 mm
Workpiece	Invar alloy

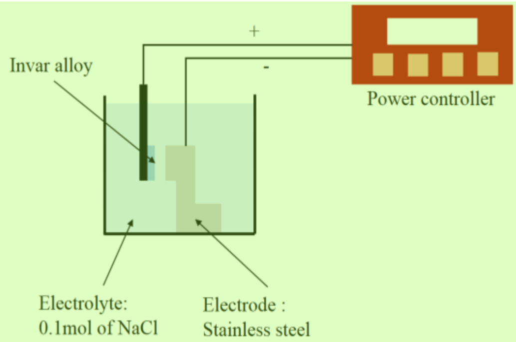

(a) Schematic

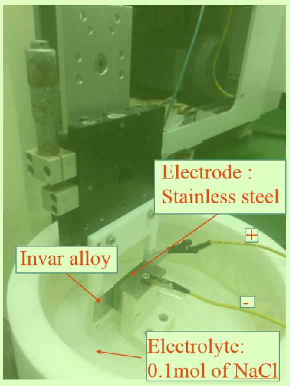

(b) Setup

Fig. 8. Schematic representation of the experiment and setup.

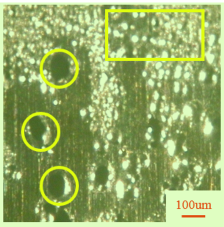

(a) 0.1 mm

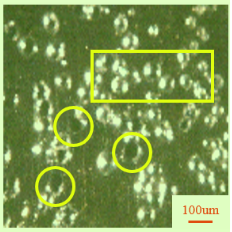

(b) 0.3 mm

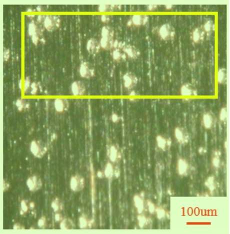

(c) 0.5 mm

Fig. 9. Result of experiment in shape electrode type.

was carry out in two types, such as the follow: Many shape electrode drilling holes using electrochemical machining and the array film mask type using electrochemical machining. Also, the machining time was 30 seconds. Unlike result of analysis, electrode gap was 0.1 mm, 0.3 mm and 0.5 mm. Because, it's changed the difference in the electrode gap in order to identify the workability trend.

Fig. 9 shows result of experiment in shape electrode type. The circle shows the holes and box shows the fitting. Fig. 9(a) shows the electrode gap was 0.1 mm. The holes were not machined regularly. Although the machining shape was not square shape, the machining zones were irregular, and the machined surface was not smooth. Figs. 9(b) and (c) shows the electrode gap was 0.3 mm and 0.5 mm. Both Figs. 9(b) and (c) is not good machined surface. In the case of Fig. 9(b), the hole is created, but hole shape was irregular. In the case of Fig. 9(c), the hole is not created. Experiment results, when the electrode gap was increased, it is confirmed that the amount of current that affect the surface is reduced. These results show good agreement with the simulations of Fig. 7(a). Also, Non-machining zones were the fitting phenomenon of irregular shape. Because of the zone where the current density between the electrode shape is duplicated.

Fig. 10 shows result of experiment in array film mask type. Fig. 10(a) shows result of the electrode gap was 0.1 mm. The holes at regular intervals, as the pattern shape was generated. However, it did not generate a hole on all patterns. Unlike the first method, Non-machined zone was not machining, and which is machined only machining zone. The result of electrochemical machining, the largest hole size was 61.054 um and the least hole size was 41.075 um. But, the machining shape was not square shape. Figs. 10(b) and (c) show the electrode gap was 0.3 mm and 0.5 mm. Both Figs. 10(b) and (c) holes at regular intervals, as the pattern shape was generated. The result of 0.3 mm, the largest hole size was 64.87 um and the least hole size was 44.837 um. and the result of 0.5 mm, the largest hole size was 58.19 um and the least hole size was 43.83 um. Fig. 10 shows the all the holes were machined alike. These results show good agreement with the simulations of Fig. 7(b). The results confirmed that the amount of current that affects the surface is the same when the electrode gap is increased.

5. Conclusion

In this study, two methods for processing Invar alloy were

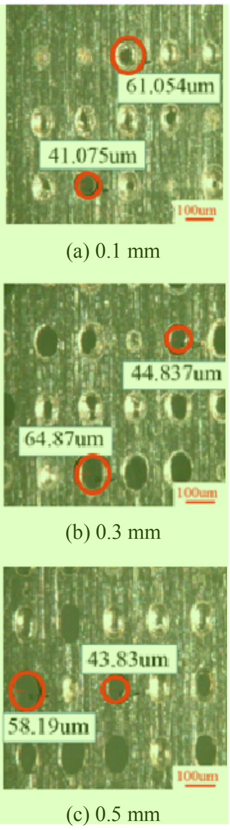

Fig. 10. Result of experiment in array film mask type.

compared. First, 2D electric field analysis was done with electrode gaps of 0.1 to 0.5 mm. the Invar alloy and electrode. In all the results of the analysis with the array film, the largest electric field value is at the edge of the electrode. When the gap was changed in the pattern type, the electric field decreased.

Second, 3D current density analysis was done for the two types of electrochemical machining. The results of the current density analysis made it possible to obtain a desired shape on Invar alloy by controlling the unnecessary current.

Finally, electrochemical machining was done using the shape electrode and array film mask. In the case of the shape electrode, the holes were irregularly processed. The machining shape was not square, the machining zones were irregular, and the machined surface was not smooth. Also, non-machining zones were the fitting phenomenon of the irregular shape. Because of the zone where the current density between the electrode shapes was duplicated. In the case of the array film, the holes were generated at regular intervals as in the pattern shape. However, holes were not generated on all patterns. Unlike the first method, the non-machined zone was not machining, which machined only the machining zone, but the machining shape was not square. The shape electrode did not achieve accurate machining due to the high current value. The array film was suitable for machining a micro-pattern on Invar alloy. However, changes in the processing conditions are required to machine exact hole shapes.

Acknowledgment

This work was supported by the National Research Foundation of Korea (NRF) grant funded by the Korea government (MSIP) (No. 2015R1A2A1A15054116).

References

[1] K. Xu, Y. Zeng, P. Li, X. Fang and D. Zhu, Effect of wire cathode surface hydrophilia when using a travelling wire in wire electrochemical micro machining, *Journal of Materials Processing Technology*, 235 (2016) 68-74.

[2] C. Xuezhen, X. Zhengyang, Z. Dong, F. Zhongding and Z. Di, Experimental research on electrochemical machining of titanium alloy Ti60 for a blisk, *Chinese Journal of Aeronautics* (2015).

[3] M. J. Shin, S. Y. Baek and E. S. Lee, A study for improving surface roughness and micro-deburring effect of nitinol shape memory alloy by electropolishing, *Transactions of the Korean Society of Machine Tool Engineers*, 16 (6) (2007) 49-54.

[4] R. Schuster, V. Kirchner, P. Allongue and G. Ertl, Electrochemical Micromachining, *Science*, 289 (2000) 98-101.

[5] E. G. Finantu-Dinu, D. Korzec, M. Teschke and J. Engemann, Influence of the electrode layout on performance of insulated surface discharge: Electrical characterization, *Surface and Coating Technology,* 174-175 (2003) 524-529.

[6] X. Chen, N. Qu, H. Li and Z. Xu, Electrochemical micromachining of micro-dimple arrays using a polydimethylsiloxane (PDMS) mask, *Journal of Materials Processing Technology*, 229 (2016) 102-110.

[7] G. Q. Wang, H. S. Li, N. S. Qu and D. Zhu, Investigation of the hole-formation process during double-sided through-mask electrochemical machining, *Journal of Materials Processing Technology*, 234 (2016) 95-101.

[8] S. Huang, X. Zhang, M. Tafu, T. Toshima and Y. Jo, Study on subway particle capture by ferromagnetic mesh filter in non-uniform magnetic field, *Separation and Purification Technology*, 156 (2005) 642-654.

[9] A. Munir, Z. Zhu, J. Wang and H. S. Zhou, FEM analysis of magnetic agitation for tagging biomolecules with magnetic nanoparticles in a microfluidic system, *Sensors and Actuators b*, 197 (2014) 1-12.

[10] X. Fang, N. Qu, Y. Zhang, Z. Xu and D. Zhu, Effects of pulsating electrolyte flow in electrochemical machining, *Journal of Materials Processing Technology*, 214 (2014) 36- 43.

Eun-Sang Lee received B.S. and M.S. degrees in Mechanical Engineering from Inha University in 1985 and in 1987. Dr. Lee received a Ph.D. from the Korea Advanced Institute of Science and Technology in 1998. Dr. Lee is currently a Professor at the School of Mechanical Engineering at Inha University in Incheon, Korea. His research fields are in ultra-precision manufacturing, electrochemical micromachining and the development of a semiconductor wafer polishing.